International Journal of
*Molecular Sciences*

MDPI

*Supporting Information*

# Pharmaceutical Cocrystals of Ethenzamide: Molecular Structure Analysis Based on Vibrational Spectra and DFT Calculations

**Mei Wan [1], Jiyuan Fang [1], Jiadan Xue [2], Jianjun Liu [1], Jianyuan Qin [1], Zhi Hong [1], Jiusheng Li [1] and Yong Du [1,*]**

[1] Centre for THz Research, China Jiliang University, Hangzhou 310018, China; wm1315286544@163.com (M.W.); jiyuanfang@foxmail.com (J.F.); jianjun@cjlu.edu.cn (J.L.); jyqin@cjlu.edu.cn (J.Q.); hongzhi@cjlu.edu.cn (Z.H.); lijsh@cjlu.edu.cn (J.L.)
[2] Department of Chemistry, Zhejiang Sci-Tech University, Hangzhou 310018, China; jenniexue@126.com
* Correspondence: yongdu@cjlu.edu.cn; Tel.: +86-571-8687-5618

**Table of Contents**

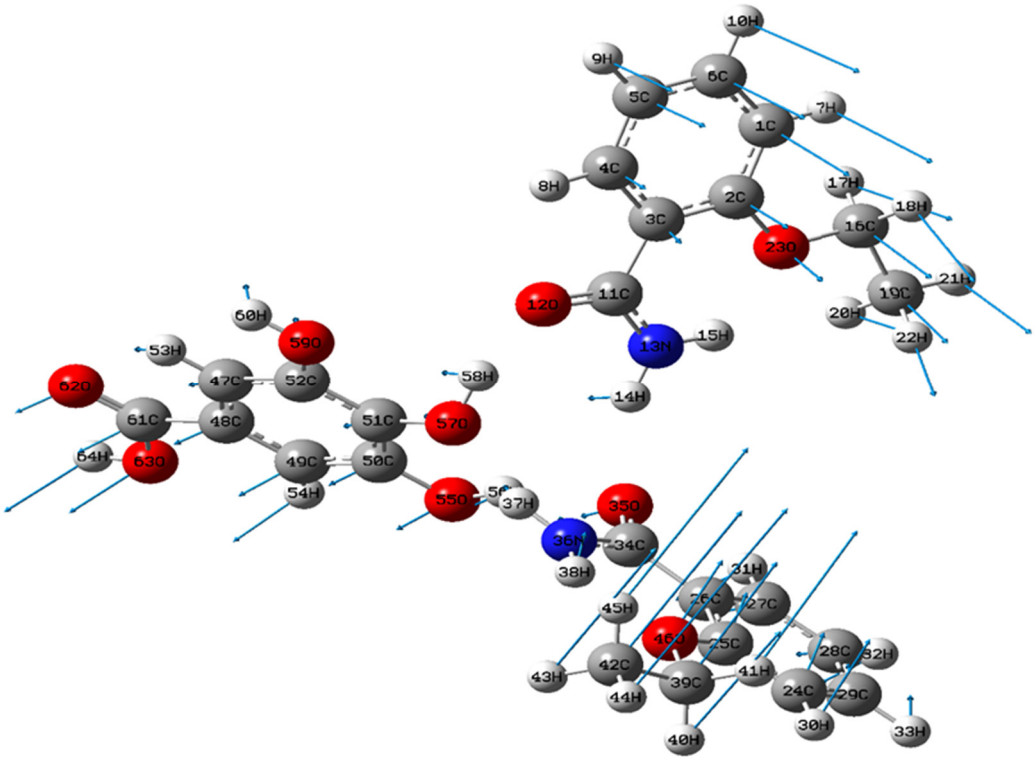


(**a**) 0.93 THz

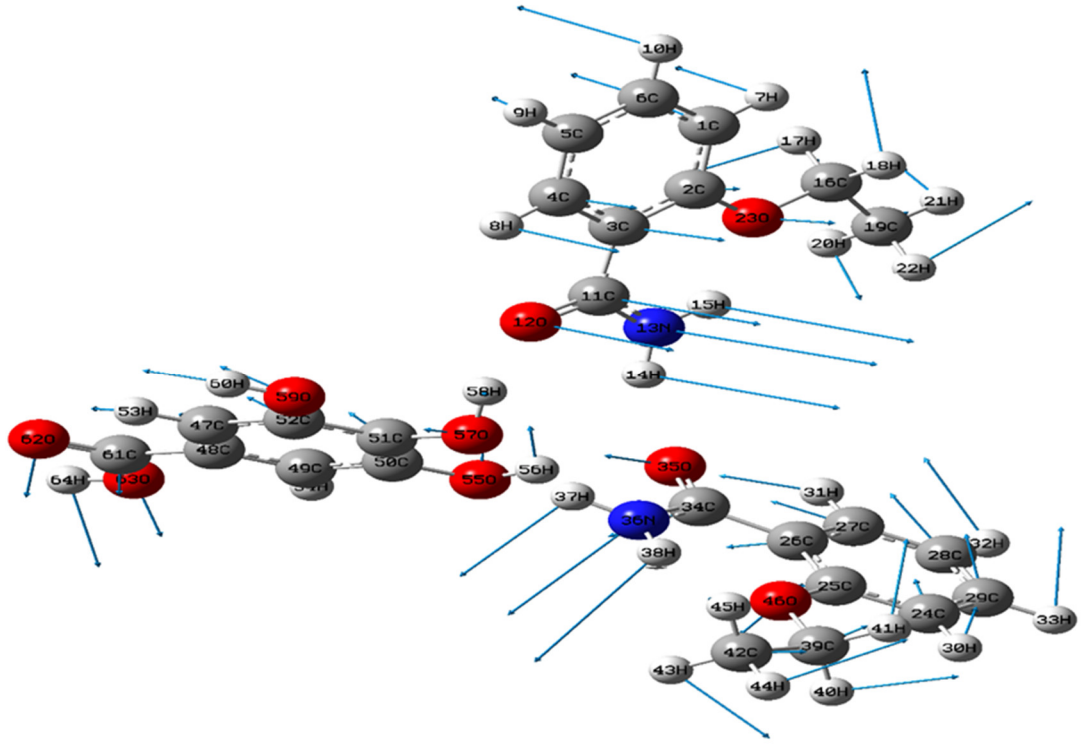


(**b**) 1.50 THz

**Figure S1.** Vibrational modes of ETZ-GA cocrystal at position of (**a**) 0.93 THz and (**b**) 1.50 THz.

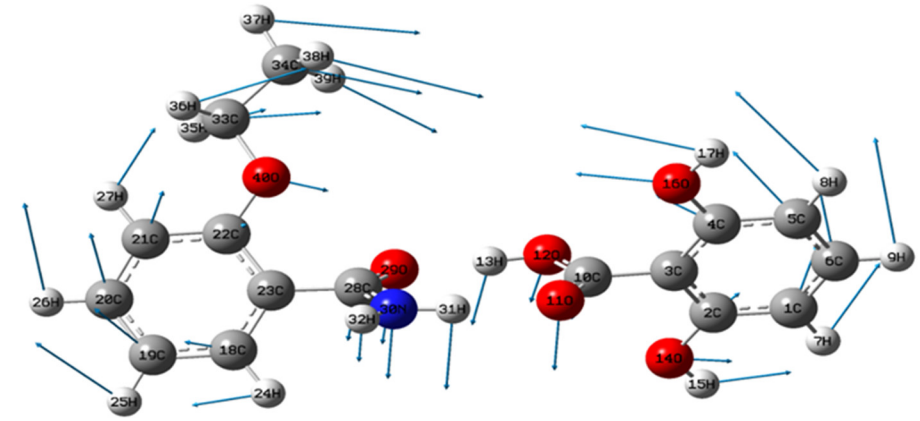


(**a**) 0.38 THz

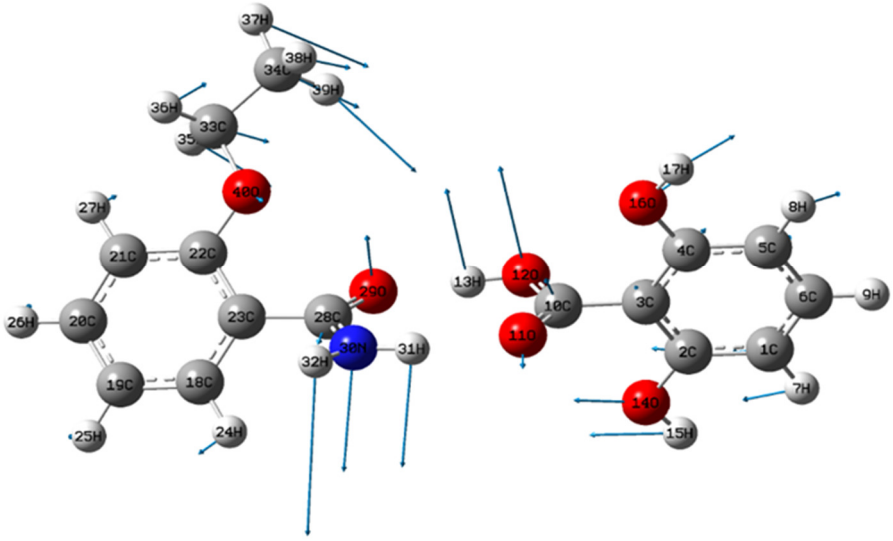


(**b**) 1.14 THz

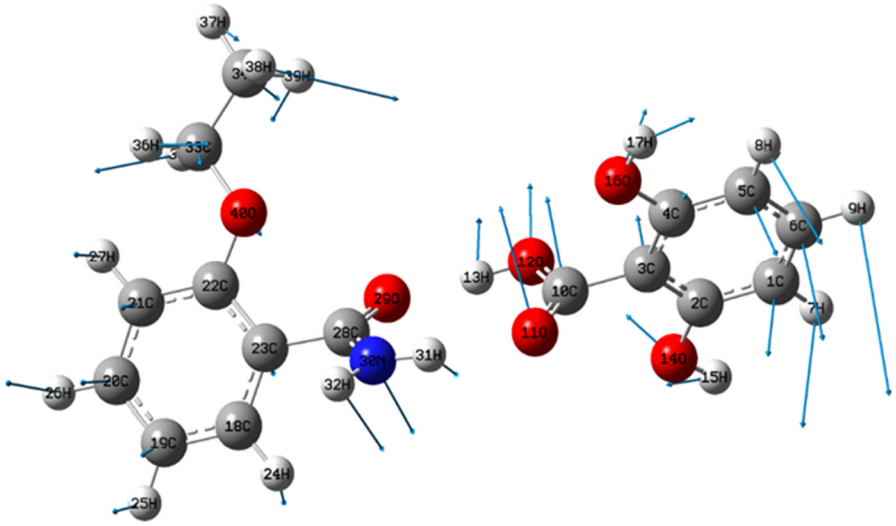


(**c**) 1.38 THz

**Figure S2.** Vibrational modes of ETZ-26DHBA cocrystal at position of (**a**) 0.38 THz, (**b**) 1.14 THz and (**c**) 1.38 THz.

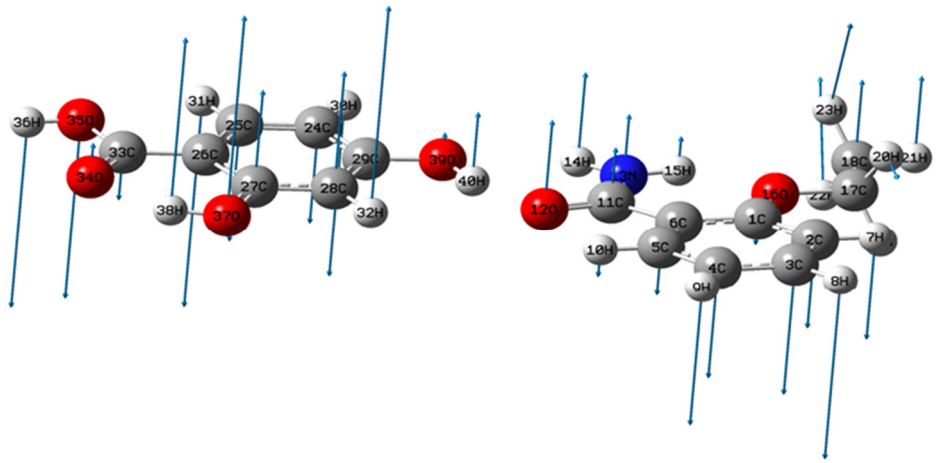

(**a**) 0.68 THz

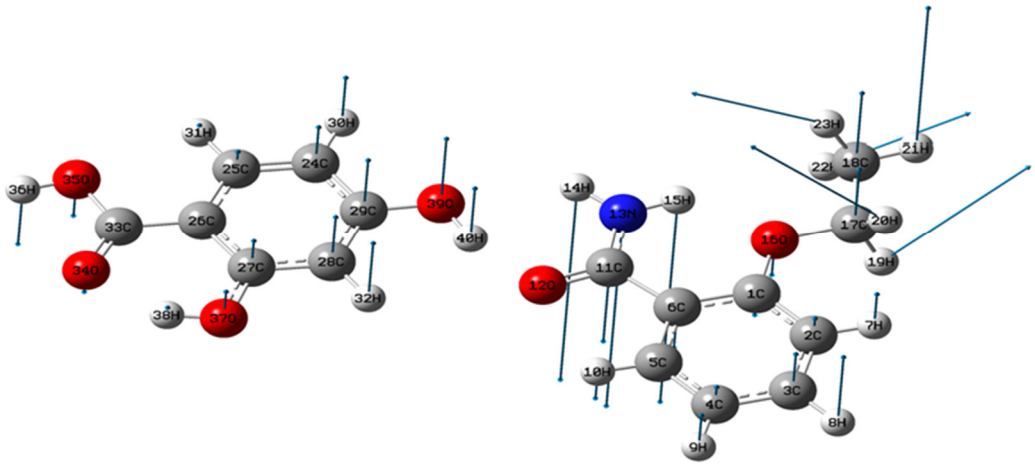

(**b**) 0.93 THz

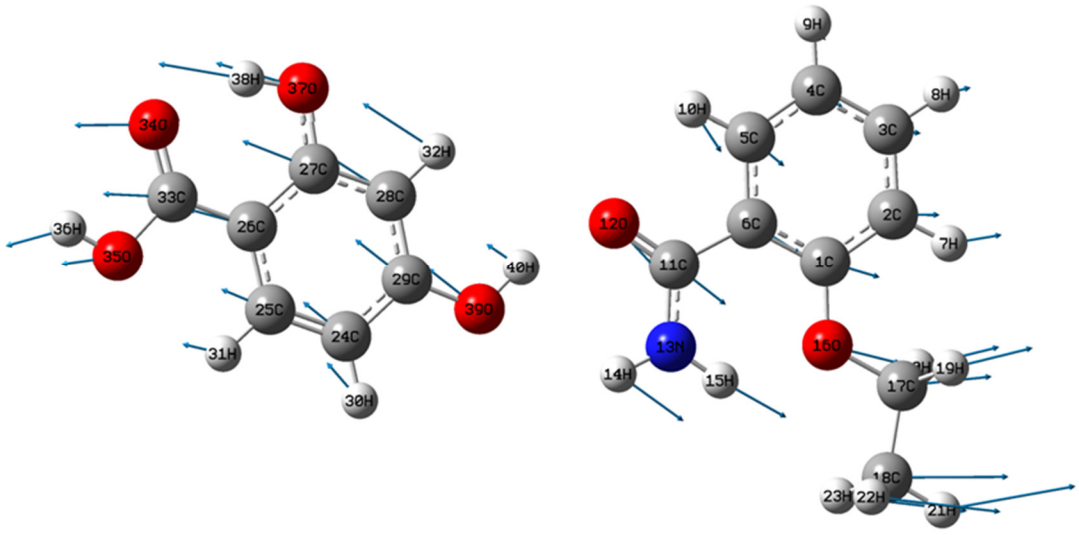

(**c**) 1.50 THz

**Figure S3.** Vibrational modes of ETZ-24DHBA cocrystal at position of (**a**) 0.68 THz, (**b**) 0.93 THz and (**c**) 1.50 THz.

**Table S1.** Comparisons of experimental and simulated THz spectral data of the ETZ cocrystals.

| Cocrystal | Experimental f/THz | Theoretical form I f/THz | Percent error | Theoretical form II f/THz | Percent error |
|---|---|---|---|---|---|
| ETZ-GA | 1.02 | 0.93 | -8.82% | 0.88 | -13.73% |
| | 1.46 | — | — | 1.41 | -3.42% |
| | 1.53 | 1.50 | -1.96% | — | |
| ETZ-26DHBA | 0.36 | 0.38 | 5.56% | 0.44 | 22.22% |
| | 1.18 | 1.14 | -3.39% | 1.21 | 2.54% |
| | 1.39 | 1.38 | -0.72% | — | — |
| ETZ-24DHBA | 0.74 | 0.55 | -25.68% | 0.68 | -8.11% |
| | 0.93 | 0.90 | -3.23% | 0.93 | 0.00% |
| | 1.20 | — | — | — | — |
| | 1.55 | — | — | 1.50 | -3.23% |

**Table S2.** Total electronic energies of the ETZ cocrystals from DFT structure simulations.

| Cocrystal | Theoretical form | Total electronic energy (hartree) |
|---|---|---|
| ETZ-GA | form I | -1756.6418 |
| | form II | -1756.6365 |
| ETZ-26DHBA | form I | -1126.4120 |
| | form II | -1266.4040 |
| ETZ-24DHBA | form I | -1126.4155 |
| | form II | -1126.4331 |

**Table S3.** Comparisons of experimental and simulated Raman spectral data of the ETZ-GA cocrystal.

| Experimental Wavenumber/cm$^{-1}$ | Theoretical Form I Wavenumber/cm$^{-1}$ | Percent Error | Theoretical Form II Wavenumber/cm$^{-1}$ | Percent Error |
|---|---|---|---|---|
| 268 | 262 | -2.24% | 258 | -3.73% |
| 345 | 327 | -5.22% | 331 | -4.06% |
| 384 | 381 | -0.78% | 377 | -1.82% |
| 426 | 428 | 0.47% | 428 | 0.47% |
| 550 | 539 | -2.00% | 543 | -1.27% |
| 615 | 632 | 2.76% | 628 | 2.11% |
| 654 | 671 | 2.60% | 671 | 2.60% |
| 704 | 694 | -1.42% | 682 | -3.13% |
| 754 | 763 | 1.19% | 767 | 1.72% |
| 793 | 790 | -0.38% | 790 | -0.38% |
| 820 | 825 | 0.61% | 833 | 1.59% |
| 928 | 937 | 0.97% | 941 | 1.40% |
| 966 | 960 | -0.62% | 964 | -0.21% |
| 1051 | 1072 | 2.00% | 1076 | 2.38% |
| 1093 | 1106 | 1.19% | 1110 | 1.56% |
| 1120 | 1145 | 2.23% | 1149 | 2.59% |
| 1167 | 1172 | 0.43% | 1176 | 0.77% |
| 1240 | 1253 | 1.05% | 1253 | 1.05% |
| 1263 | 1299 | 2.85% | 1303 | 3.17% |
| 1309 | 1330 | 1.60% | 1334 | 1.91% |
| 1375 | 1365 | -0.73% | 1361 | -1.02% |
| 1421 | 1396 | -1.76% | 1403 | -1.27% |
| 1460 | 1484 | 1.64% | 1488 | 1.92% |
| 1533 | 1562 | 1.89% | 1558 | 1.63% |
| 1606 | 1596 | -0.62% | 1600 | -0.37% |
| 1633 | 1635 | 0.12% | 1635 | 0.12% |
| 1687 | 1673 | -0.83% | 1670 | -1.01% |
| 1745 | 1743 | -0.11% | 1739 | -0.34% |
| | RMSE | 15.83 | RMSE | 17.30 |

RMSE: root mean square error.

**Table S4.** Comparisons of experimental and simulated Raman spectral data of the ETZ-26DHBA cocrystal.

| Experimental Wavenumber/cm$^{-1}$ | Theoretical Form I Wavenumber/cm$^{-1}$ | Percent error | Theoretical form II wavenumber/cm$^{-1}$ | Percent Error |
|---|---|---|---|---|
| 256 | 227 | -11.33% | 227 | -11.33% |
| 291 | 262 | -9.97% | 250 | -14.09% |
| 345 | 327 | -5.22% | 316 | -8.41% |
| 403 | 370 | -8.19% | 339 | -15.88% |
| 434 | 420 | -3.23% | 431 | -0.69% |
| 565 | 536 | -5.13% | 543 | -3.89% |
| 600 | 597 | -0.50% | 597 | -0.50% |
| 708 | 736 | 3.95% | 736 | 3.95% |
| 754 | 763 | 1.19% | 763 | 1.19% |
| 827 | 825 | -0.24% | 825 | -0.24% |
| 931 | 941 | 1.07% | 937 | 0.64% |
| 1059 | 1068 | 0.85% | 1110 | 4.82% |
| 1120 | 1133 | 1.16% | 1153 | 2.95% |
| 1163 | 1180 | 1.46% | 1180 | 1.46% |
| 1201 | 1214 | 1.08% | 1211 | 0.83% |
| 1286 | 1280 | -0.47% | 1249 | -2.88% |
| 1307 | 1307 | 0.00% | 1311 | 0.31% |
| 1363 | 1361 | -0.15% | 1361 | -0.15% |
| 1390 | 1415 | 1.80% | 1423 | 2.37% |
| 1464 | 1492 | 1.91% | 1492 | 1.91% |
| 1541 | 1530 | -0.71% | 1596 | 3.57% |
| 1603 | 1616 | 0.81% | 1619 | 1.00% |
| 1649 | 1639 | -0.61% | 1646 | -0.18% |
| 1695 | 1704 | 0.53% | 1689 | -0.35% |
| 1745 | 1751 | 0.34% | 1751 | 0.34% |
| | RMSE | 17.63 | RMSE | 27.98 |

RMSE: root mean square error.

**Table S5.** Comparisons of experimental and simulated Raman spectral data of the ETZ-24DHBA cocrystal.

| Experimental wavenumber / $cm^{-1}$ | Theoretical form I wavenumber / $cm^{-1}$ | Percent error | Theoretical form II wavenumber / $cm^{-1}$ | Percent error |
|---|---|---|---|---|
| 276 | 277 | 0.36% | 281 | 1.81% |
| 299 | 308 | 3.01% | 312 | 4.35% |
| 334 | 335 | 0.30% | 339 | 1.50% |
| 384 | 385 | 0.26% | 385 | 0.26% |
| 418 | 416 | -0.48% | 420 | 0.48% |
| 480 | 439 | -8.54% | 454 | -5.42% |
| 526 | 524 | -0.38% | 539 | 2.47% |
| 611 | 547 | -10.47% | 617 | 0.98% |
| 638 | 632 | -0.94% | 632 | -0.94% |
| 754 | 694 | -7.96% | 763 | 1.19% |
| 781 | 759 | -2.82% | 786 | 0.64% |
| 823 | 825 | 0.24% | 825 | 0.24% |
| 928 | 937 | 0.97% | 937 | 0.97% |
| 978 | 998 | 2.04% | 995 | 1.74% |
| 1051 | 1072 | 2.00% | 1072 | 2.00% |
| 1093 | 1110 | 1.56% | 1110 | 1.56% |
| 1159 | 1137 | -1.90% | 1141 | -1.55% |
| 1194 | 1211 | 1.42% | 1180 | -1.17% |
| 1236 | 1249 | 1.05% | 1199 | -2.99% |
| 1271 | 1303 | 2.52% | 1249 | -1.73% |
| 1333 | 1353 | 1.50% | 1338 | 0.38% |
| 1398 | 1400 | 0.14% | 1396 | -0.14% |
| 1464 | 1492 | 1.91% | 1492 | 1.91% |
| 1556 | 1623 | 4.31% | 1546 | -0.64% |
| 1595 | 1654 | 3.70% | 1616 | 1.32% |
| 1637 | 1688 | 3.12% | 1662 | 1.53% |
| 1726 | 1750 | 1.39% | 1712 | -0.81% |
| | RMSE | 30.73 | RMSE | 15.98 |

RMSE: root mean square error.

**Table S6.** Vibrational modes for characteristic peaks of the ETZ-GA cocrystal in Raman spectra.

| Mode | Theoretical wavenumber / $cm^{-1}$ | Experimental wavenumber / $cm^{-1}$ | Mode assignment |
|---|---|---|---|
| $\nu_1$ | 262 | 268(w) | ρ(H17-C16-H18, O12=C11-N13-H14) |
| $\nu_2$ | 327 | 345(w) | δ(O62=C61-O63-H64), ρ(H37-N36-H38, H40-C39-H41) |
| $\nu_3$ | 381 | 384(w) | Def(R2), ρ(H37-N36-H38, H40-C39-H41) |
| $\nu_4$ | 428 | 426(m) | Def(R2), Def(R3), ρ(O62=C61-O63-H64) |
| $\nu_5$ | 539 | 550(m) | ω(H15-N13-C11, H37-N36-H38), Def(R1) |
| $\nu_6$ | 632 | 615(w) | ρ(H37-N36-H38, H14-N13-H15), Def(R2) |
| $\nu_7$ | 671 | 654(m) | δ(O62=C61-O63-H64), Def(R3) |
| $\nu_8$ | 694 | 704(m) | τ(H14-N13-H15), Def(R1) |
| $\nu_9$ | 763 | 754(w) | Def(R2), ρ(H14-N13-H15, H37-N36-H38) |
| $\nu_{10}$ | 790 | 793(s) | Def(R3), δ(O62=C61-O63-H64), ρ(H37-N36-H38) |
| $\nu_{11}$ | 825 | 820(s) | ρ(H37-N36-H38, H40-C39-H41), Def(R2) |
| $\nu_{12}$ | 937 | 928(w) | Def(R2), ρ(H37-N36-H38, H40-C39-H41) |
| $\nu_{13}$ | 960 | 966(vw) | Def(R3), δ(O62=C61-O63-H64) |
| $\nu_{14}$ | 1072 | 1051(m) | Def(R2) |
| $\nu_{15}$ | 1106 | 1093(m) | Def(R1), ρ(H14-N13-H15) |
| $\nu_{16}$ | 1145 | 1120(m) | ρ(H14-N13-H15, H37-N36-H38) |
| $\nu_{17}$ | 1172 | 1167(m) | ρ(H37-N36-H38), Def(R2) |
| $\nu_{18}$ | 1253 | 1240(w) | Def(R2), ρ(H37-N36-H38), θ(C25-O46) |
| $\nu_{19}$ | 1299 | 1263(s) | Def(R1), ρ(H14-N13-H15, H37-N36-H38) |
| $\nu_{20}$ | 1330 | 1309(s) | Def(R2) |
| $\nu_{21}$ | 1365 | 1375(s) | δ(H37-N36-H38), Def(R3) |
| $\nu_{22}$ | 1396 | 1421(w) | Def(R3), δ(O62=C61-O63-H64) |
| $\nu_{23}$ | 1484 | 1460(m) | Def(R2), δ(H40-C39-H41) |
| $\nu_{24}$ | 1562 | 1533(m) | Def(R3), ρ(O62=C61-O63-H64) |
| $\nu_{25}$ | 1596 | 1606(s) | θ(C34=O35), Def(R2), δ(H14-N13-H15, H37-N36-H38) |
| $\nu_{26}$ | 1635 | 1633(s) | θ(C11=O12), Def(R1), Def(R3), ρ(H37-N36-H38) |
| $\nu_{27}$ | 1673 | 1687(m) | θ(C34=O35), δ(H14-N13-H15, H37-N36-H38) |
| $\nu_{28}$ | 1743 | 1745(m) | θ(C61=O62), Def(R3) |

Vw-very weak, w-weak, m-medium, s-strong, θ-stretching, ρ-in-plane rocking vibration, δ-scissor, ω-out of plane rocking vibration, τ-torsion, Def-Deformation.

**Table S7.** Vibrational modes for characteristic peaks of the ETZ-26DHBA cocrystal in Raman spectra.

| Mode | Theoretical wavenumber / $cm^{-1}$ | Experimental wavenumber / $cm^{-1}$ | Mode assignment |
|---|---|---|---|
| $\nu_1$ | 227 | 256(m) | τ(H31-N30-H32), ρ(O11=C10-O12-H13), ω(O29=C28-N30-H31) |
| $\nu_2$ | 262 | 291(m) | ρ(H31-N30-H32, O11=C10-O12-H13, H35-C33-H36) |
| $\nu_3$ | 327 | 345(w) | Def(R1), ρ(O11=C10-O12-H13, H35-C33-H36) |
| $\nu_4$ | 370 | 403(m) | Def(R1), ρ( H31-N30-H32, H35-C33-H36) |
| $\nu_5$ | 420 | 434(m) | ρ(O11=C10-O12-H13), Def(R2), δ(O34=C33-O35-H36, H26-C20=C21-H27) |
| $\nu_6$ | 536 | 565(m) | ρ(O11=C10-O12-H13), Def(R2) |
| $\nu_7$ | 597 | 600(m) | δ(O11=C10-O12-H13), Def(R2) |
| $\nu_8$ | 736 | 708(m) | Def(R2), δ(O11=C10-O12-H13), ρ(H31-N30-H32) |
| $\nu_9$ | 763 | 754(s) | Def(R1), ρ(H31-N30-H32) |
| $\nu_{10}$ | 825 | 827(w) | Def(R1), δ(O11=C10-O12-H13), ρ(H31-N30-H32) |
| $\nu_{11}$ | 941 | 931(w) | Def(R1), ρ(H35-C33-H36) |
| $\nu_{12}$ | 1068 | 1059(s) | Def(R1) |
| $\nu_{13}$ | 1133 | 1120(m) | ρ(H31-N30-H32, H35-C33-H36), δ(H24-C18=C19-H25) |
| $\nu_{14}$ | 1180 | 1163(s) | δ(H7-C1=C6-H9, H8-C5=C6-H9) |
| $\nu_{15}$ | 1214 | 1201(m) | Def(R2), θ(C10=O12) |
| $\nu_{16}$ | 1280 | 1286(s) | θ(C22-O40), Def(R1) |
| $\nu_{17}$ | 1307 | 1307(m) | ρ(H26-C20=C21-H27, H24-C18=C19-H25, H35-C33-H36) |
| $\nu_{18}$ | 1361 | 1363(w) | Def(R2) |
| $\nu_{19}$ | 1415 | 1390(w) | Def(R1), δ(H31-N30-C28) |
| $\nu_{20}$ | 1492 | 1464(w) | θ(C2-O14, C4-O16), Def(R2) |
| $\nu_{21}$ | 1530 | 1541(m) | δ(H35-C33-H36), Def(R1) |
| $\nu_{22}$ | 1616 | 1603(s) | δ(H31-N30-H32), Def(R1), θ(C28=O29) |
| $\nu_{23}$ | 1639 | 1649(m) | δ(H31-N30-H32), Def(R1) |
| $\nu_{24}$ | 1704 | 1695(vw) | θ(C28=O29, C10=O11), δ( H31-N30-H32) |
| $\nu_{25}$ | 1751 | 1745(vw) | θ(C28=O29, C10=O11), ρ(H31-N30-H32) |

Vw-very weak, w-weak, m-medium, s-strong, θ-stretching, ρ-in-plane rocking vibration, δ-scissor, ω-out of plane rocking vibration, τ-torsion, Def-Deformation.

**Table S8.** Vibrational modes for characteristic peaks of the ETZ-24DHBA cocrystal in Raman spectra.

| Mode | Theoretical wavenumber / $cm^{-1}$ | Experimental wavenumber / $cm^{-1}$ | Mode assignment |
|---|---|---|---|
| $\nu_1$ | 281 | 276(w) | δ(C11-C6=C1, C33-C26=C1) |
| $\nu_2$ | 312 | 299(w) | ρ(H15-N13-H14, H20-C17-H19, H23-C18-H22) |
| $\nu_3$ | 339 | 334(w) | ρ(H20-C17-H19, H23-C18-H22), Def(R1), δ(C33-C26=C1) |
| $\nu_4$ | 385 | 384(m) | δ(O34=C33-O35-H36, C11-C6=C5), Def(R1), ρ(H15-N13-H14, H23-C18-H22) |
| $\nu_5$ | 420 | 418(m) | ρ(O34=C33-O35-H36, H20-C17-H19, H23-C18-H22), Def(R2) |
| $\nu_6$ | 454 | 480(w) | ρ(O34=C33-O35-H36), δ(C11-C6=C5), Def(R1) |
| $\nu_7$ | 539 | 526(m) | ρ(H15-N13-H14), δ(O34=C33-O35-H36), Def(R1) |
| $\nu_8$ | 617 | 611(m) | ρ(C11-C6=C1), δ(O34=C33-O35-H36), Def(R1), |
| $\nu_9$ | 632 | 638(w) | Def(R2), ρ(H15-N13-H14) |
| $\nu_{10}$ | 763 | 754(s) | Def(R1), δ(O34=C33-O35-H36) |
| $\nu_{11}$ | 786 | 781(s) | ω(H8-C3=C2-H7, O12=C11-C6), τ(H15-N13-C11) |
| $\nu_{12}$ | 825 | 823(w) | ρ(H15-N13-H14), Def(R2) |
| $\nu_{13}$ | 937 | 928(vw) | Def(R2) |
| $\nu_{14}$ | 995 | 978(m) | Def(R1) |
| $\nu_{15}$ | 1072 | 1051(m) | Def(R2) |
| $\nu_{16}$ | 1110 | 1093(m) | ρ(H15-N13-H14), Def(R2) |
| $\nu_{17}$ | 1141 | 1159(m) | ρ(H15-N13-H14) |
| $\nu_{18}$ | 1180 | 1194(w) | ω(O16-C17-C18), ρ(H20-C17-H19) |
| $\nu_{19}$ | 1199 | 1236(s) | ρ(H31-C25=C24-H30, C33-C26=C27) |
| $\nu_{20}$ | 1249 | 1271(s) | θ(C1-O16), Def(R2), δ(H8-C3=C4-H9) |
| $\nu_{21}$ | 1338 | 1333(s) | ρ(H31-C25=C24-H30), δ(C33-C26=C27), Def(R1) |
| $\nu_{22}$ | 1396 | 1398(w) | Def(R1), δ(C11-N13-H14), ρ(H8-C3=C4-H9, H31-C25=C24-H30) |
| $\nu_{23}$ | 1492 | 1464(m) | θ(C27-O37), ρ(H8-C3=C4-H9), Def(R1) |
| $\nu_{24}$ | 1546 | 1556(m) | Def(R1), ρ(H31-C25=C24-H30), θ(C27=C26) |
| $\nu_{25}$ | 1616 | 1595(s) | Def(R2), δ(H15-N13-H14) |
| $\nu_{26}$ | 1662 | 1637(s) | θ(C25=C24, C28=C27, C33=O34), Def(R1) |
| $\nu_{27}$ | 1712 | 1726(m) | θ(C33=O34, C11=O12), δ(H15-N13-H14) |

Vw-very weak, w-weak, m-medium, s-strong, θ-stretching, ρ-in-plane rocking vibration, δ-scissor, ω-out of plane rocking vibration, τ-torsion, Def-Deformation.